Eur. Phys. J. A **11**, 113–119 (2001)

THE EUROPEAN PHYSICAL JOURNAL A

Production of a_0^+-mesons in the reaction $pp \to da_0^+$

H. Müller[a]

Institut für Kern- und Hadronenphysik, Forschungszentrum Rossendorf, Postfach 510119, 01314 Dresden, Germany

Received: 20 December 2000 / Revised version: 7 May 2001
Communicated by M. Garçon

Abstract. We investigate the reaction $pp \to da_0^+$ at COSY and SIS energies together with accompanying background reactions and inclusive particle yields. The a_0^+ is considered as a usual $u\bar{d}$ quark model state with two decay channels $a_0^+ \to K^+\bar{K}^0$ and $a_0^+ \to \pi^+\eta$. Calculated cross-sections for a_0^+ production as well as for the corresponding non-resonant channels $pp \to dK^+\bar{K}^0$ and $pp \to d\pi^+\eta$ are compared. Especially, in case of the final channel $d\pi^+\eta$, high statistics measurements are necessary to extract the a_0^+ signal from the high non-resonant background.

PACS. 13.75.Cs Nucleon-nucleon interactions (including antinucleons, deuterons, etc.) – 13.25.-k Hadronic decays of mesons

1 Introduction

The structure of the lightest scalar mesons $a_0(980)$ and $f_0(980)$ is not well understood (see the "note on scalar mesons" of the particle data group (PDG) [1] and references therein). Several options concerning the nature of the a_0-meson are at present under discussion. For example, the a_0 has been proposed to be a $K\bar{K}$ bound state, a multi-quark state or a vacuum scalar. For a more thorough discussion on this topic the interested reader is referred to a recent paper [2], where the reactions $\pi N \to a_0 N$ and $pp \to da_0^+$ have been investigated. The authors [2] have emphasized the necessity of new measurements of both the a_0 production and the a_0 branching ratios for clarifying the a_0 structure. Such an experiment, which aims at detecting the a_0^+ in the two main decay modes in the reaction $pp \to da_0^+$, is presently prepared at COSY (Jülich) [3]. It is planned to measure the d in coincidence with either the K^+ or the π^+. By setting a window in the missing mass spectrum on the mass of the corresponding third particle, the $\bar{K}^0$ or the η, the final channel to be measured is fixed. The a_0^+ should be then visible in the invariant mass distributions of its decay channels $K^+ + \bar{K}^0$ and $\pi^+ + \eta$.

In [2] predictions for the reaction $pp \to da_0^+$ at COSY energies have been given. But no attempts have been made so far to compare the channels with a_0^+ production and subsequent decays, namely $pp \to da_0^+ \to dK^+\bar{K}^0$ and $pp \to da_0^+ \to d\pi^+\eta$, with the non-resonant channels $pp \to dK^+\bar{K}^0$ and $pp \to d\pi^+\eta$. For the measurement of a_0^+ production the latter channels might be rather disturbing if they are of high intensity. Therefore, an estimate of the non-resonant cross-sections seems to be desirable. Another source of background are multi-pion channels, where two or three pions may have an invariant mass similar to the η mass. Furthermore, for beam time estimates it is useful to compare the inclusive particle yields with the yields from a_0^+ production. These are the points we intend to deal with in the present paper. As in [2] we compare the results of our calculations with the available data on the cross-sections of the reaction $pp \to da_0^+$ [4] at beam momenta 3.8, 4.5 and 6.3 GeV/c. Then we predict the cross-sections for a_0^+ production *together* with an estimate of the cross-sections for the non-resonant and the multi-pion channels at COSY and SIS energies. Implications on the feasibility of the proposed measurements are discussed.

The calculations of the reaction $pp \to da_0^+$ in [2] were carried out on the basis of an effective Lagrangian approach and the Regge pole model in conjunction with the two-step model. Here we use a completely different approach, namely the Rossendorf collision (ROC) model [5–12], which is implemented as an event generator sampling complete events. This offers the possibility to derive the contributions from all channels of interest on the basis of a unified approach. It should be noted, however, that at low energies a basically statistical approach like the ROC model cannot be expect to yield the precision of models usually based on the consideration of various types of diagrams and tailored to describe selected channels in limited energy regions above threshold. Nevertheless, the possibility to get at least an order of magnitude estimate of *all* channels relevant for a planned experiment is important for optimizing the measurements. A detailed description of the latest version of the ROC model can be found in

[a] e-mail: H.Mueller@fz-rossendorf.de

[12], where it has been applied for the interpretation of soft multi-particle production in the c.m. energy region up to ISR energies. Earlier applications to pp and pA reactions at low energies are described in [5–11].

The paper is organized as follows. In sect. 2 the features of the ROC model relevant for the present considerations are explained. Section 3 contains a comparison of experimental data with model calculations in order to give an impression concerning the applicability and accuracy of the ROC model in the near threshold region. Then, the feasibility of the measurement of the a_0^+ branching ratios into the two main channels is discussed in sect. 4 on the basis of ROC model predictions. Conclusions are summarized in sect. 5.

2 The model

In the ROC model hadrons are considered as composite objects consisting of partons. The interaction proceeds via parton-parton collisions from which a varying number of intermediate excited subsystems, called fireballs (FB), emerge together with the remnants of the initial hadrons. These subsystems decay after the collision into the primary hadrons via the creation of quark pairs with subsequent random combination to hadrons. Resonances among the primary hadrons decay until a final state consisting of stable hadrons is reached.

The ROC model is based on a modified statistical approach where the dynamics of the interaction is implemented in form of empirical functions which either suppress certain regions of the phase space or impose additional non-statistical weights. We define a channel α by the number n, masses m_i and quantum numbers of the final particles. The relative probability of populating a channel α is calculated as the product of the Lorentz-invariant phase-space factor $\mathrm{d}L_n(s;\alpha)$ with the square of an empirical matrix element A^2, which describes the dynamics of the interaction process:

$$\mathrm{d}W(s;\boldsymbol{\alpha}_N) \propto \mathrm{d}L_n(s;\boldsymbol{\alpha}_N)\, A^2 \,. \tag{1}$$

Here, $s = p^2$ denotes the square of the total energy with p being the total four-momentum. The square of the matrix element A^2,

$$A^2 = A_\mathrm{i}^2 A_\mathrm{qs}^2 A_\mathrm{ex}^2 A_\mathrm{t}^2 A_\mathrm{l}^2 A_\mathrm{st}^2 \,, \tag{2}$$

describes the interaction A_i^2 resulting in the production of a varying number N of FBs, the production of hadrons A_qs^2 via the creation of quark-anti-quark ($q\bar{q}$) pairs , the invariant mass distribution of the FBs A_ex^2, the transverse A_t^2 and longitudinal A_l^2 momentum distribution of the FBs, and, finally, some additional factors A_st^2 necessary for the calculation of the statistical weights. A more thorough description of the matrix element together with a table of parameter values can be found in [12]. Here we use the same parameter set without any changes. The cross-section is written as

$$\mathrm{d}\sigma(s) = \sigma_\mathrm{in}(s) \frac{\mathrm{d}W(s;\boldsymbol{\alpha}_N)}{\sum_N \sum_{\boldsymbol{\alpha}_N} \int \mathrm{d}W(s;\boldsymbol{\alpha}_N)} \,, \tag{3}$$

where the inelastic cross-section $\sigma_\mathrm{in}(s)$ of the considered reaction serves as normalization. Any physical quantity of interest can be derived from (3) by summing the contributions from all channels and integrating over the unobserved variables.

Deuteron production is considered in the ROC model as final-state interaction. According to the basic ideas of the coalescence model (see, *e.g.*, [13] and references therein) a proton and a neutron may coalesce into a deuteron if they are close enough in momentum space. In the context of the ROC model we compare the number of states of a free proton-neutron pair having relative momentum $\mathbf{q}$

$$\mathrm{d}\mathcal{Z}_{pn} = \mathrm{d}^3q\; V_{pn}(2\sigma_N+1)^2 \tag{4}$$

and the corresponding overlap with the square of the deuteron wave function $\Psi_d(q)$

$$\mathrm{d}\mathcal{Z}_d = \mathrm{d}^3q\; |\Psi_d(q)|^2(2\sigma_d+1)\,. \tag{5}$$

The factors $(2\sigma_N+1)^2$ and $(2\sigma_d+1)$ are the numbers of spin states of the two-nucleon system and the deuteron, respectively. We neglect off-shell effects and derive from (4) and (5) the probability for deuteron formation

$$\begin{aligned} W_d(q) &= \mathrm{d}\mathcal{Z}_d/(\mathrm{d}\mathcal{Z}_d + \mathrm{d}\mathcal{Z}_{pn}) \\ &= \frac{|\Psi_d(q)|^2(2\sigma_d+1)}{|\Psi_d(q)|^2(2\sigma_d+1) + V_{pn}(2\sigma_N+1)^2}\,. \end{aligned} \tag{6}$$

For the radius of the normalization volume V_{pn} the value $R = 1.29\,\mathrm{fm}$ from the parameter table of [12] is used.

It should be noted that nearly identical results are achieved if the probability for coalescence is approximated by a Gaussian

$$W_d(M_{np}) = \frac{2\sigma_d+1}{(2\sigma_N+1)^2} \exp\left[-\left(\frac{(M_{np}-m_n-m_p)}{c_d}\right)^2\right], \tag{7}$$

where M_{np} denotes the invariant mass of the proton-neutron pair, and m_n and m_p are the rest masses of the proton and the neutron, respectively. The parameter $c_d = 0.04\,\mathrm{GeV}$ is adjusted to reasonably reproduce the energy dependence of the reaction $pp \to d\pi^+$. A generalization of (7) to the coalescence of more than two nucleons to fragments is straightforward. This feature is important for the application of the ROC model to nuclear reactions. For the present calculations we use, however, eq. (6) with the Paris deuteron wave function [14].

Primary hadrons are formed by randomly combining quarks. For given quark flavors an empirical probability distribution,

$$W_\mathrm{h}(m_\mathrm{h}) \propto \exp\left[-m_\mathrm{h}/\Theta_\mathrm{h}\right], \tag{8}$$

with the parameter $\Theta_\mathrm{h} = 0.25\,\mathrm{GeV}$, is used to suppress the formation of the heavier hadrons of mass m_h. During event generation the masses of resonances are sampled according to a probability distribution consisting of the product of a

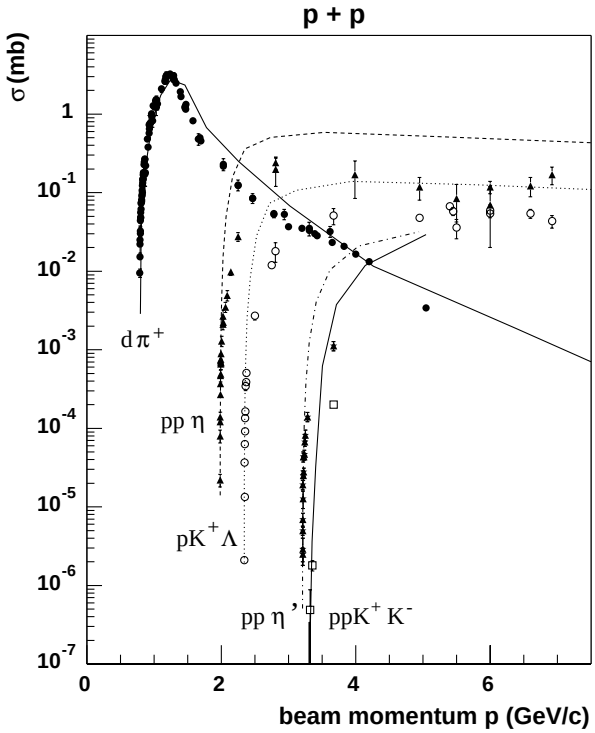

Fig. 1. Momentum dependence of the cross-sections for the reactions $pp \to d\pi^+$, $pp \to pp\eta$, $pp \to pK^+\Lambda$, $pp \to pp\eta'$ and $pp \to ppK^+K^-$. Experimental data (symbols) from [15–30] are compared with ROC model calculations (lines).

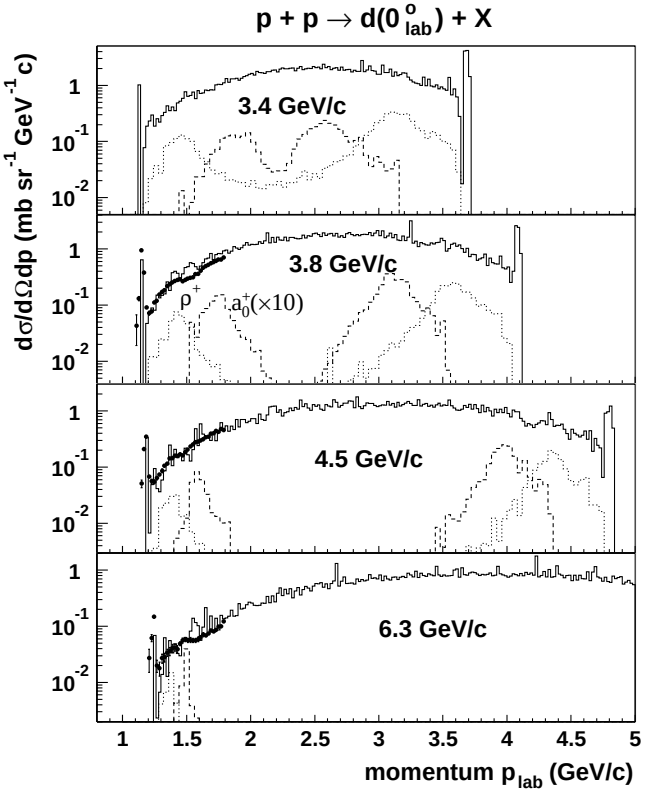

Fig. 2. Deuteron laboratory momentum spectra at four incident momenta. The data [4] for 3.8, 4.5 and 6.3 GeV/c (dots) are compared with ROC model calculations (full histograms) carried out with a cut for the polar angle of $\Theta \leq 3.6°$. Contributions from the reactions $pp \to da_0^+$ and $pp \to d\rho^+$ are shown by the dashed and dotted histograms, respectively. The contributions from $pp \to da_0^+$ are multiplied by a factor of 10.

relativistic Breit-Wigner distribution, the phase space factor of the decay products and the above suppression factor $W_{\rm h}(m_{\rm h})$. The a_0^+-meson is considered as a quark-model state, which is formed from the recombination of two light quarks according to $u\bar{d} \to a_0^+$. Its mass and width parameters of the Breit-Wigner distribution are assumed to be 0.9835 GeV and 0.075 GeV, respectively. The assumed width is the mean of the interval 50 . . . 100 MeV estimated by the PDG [1]. For the two channels $a_0^+ \to K^+\bar{K}^0$ and $a_0^+ \to \pi^+\eta$ relative decay probabilities of 30% and 70% are taken in the present calculations. The $\pi\eta$ mode is quoted by the PDG [1] as "dominant", the $K\bar{K}$ mode as "seen". The results of the calculations presented in the following sections strongly depend on the above assumptions.

3 Comparison with data

In the present section experimental data in the near threshold region are compared with ROC model calculations. The aim of this comparison with known data consists in demonstrating the ability of the model to reproduce different exclusive cross-sections even in the threshold region on the basis of a unified approach. This approach is then believed to be able to estimate at least the order of magnitude of still unknown cross-sections necessary to discuss the reaction $pp \to da_0^+$ in sect. 4.

In [8] an earlier version of the ROC model was applied to describe the energy dependence of a large variety of inclusive as well as exclusive reaction channels with two up to eight final particles in the energy region between threshold and about 50 GeV/c. The present version of the ROC model yields quite similar results for all these channels. A few of them are once more considered in fig. 1, because new experimental data in the threshold region are now available from SATURNE, CELSIUS and COSY. One feature common to all the considered channels is the overestimation of the cross-sections at c.m. energies around 100 MeV above threshold. A possible explanation might be the neglect of final-state interactions between the final particles. The largest deviations of about one order of magnitude occur at 3.67 GeV/c for the reactions $pp \to pp\eta'$ and $pp \to ppK^+K^-$ measured with DISTO [29,27]. Nevertheless, taking into account that we use a common parameter set for the whole energy region between threshold and ISR energies and that we calculate all reactions within one unified approach, the reproduction of the data near threshold is reasonably good. Of course, the achieved accuracy cannot compete with approaches describing selected channels in limited energy regions (see *e.g.* [23,31–33, and references therein]).

The data of [4] are of special interest for the consideration of a_0 production. There, differential cross-sections for

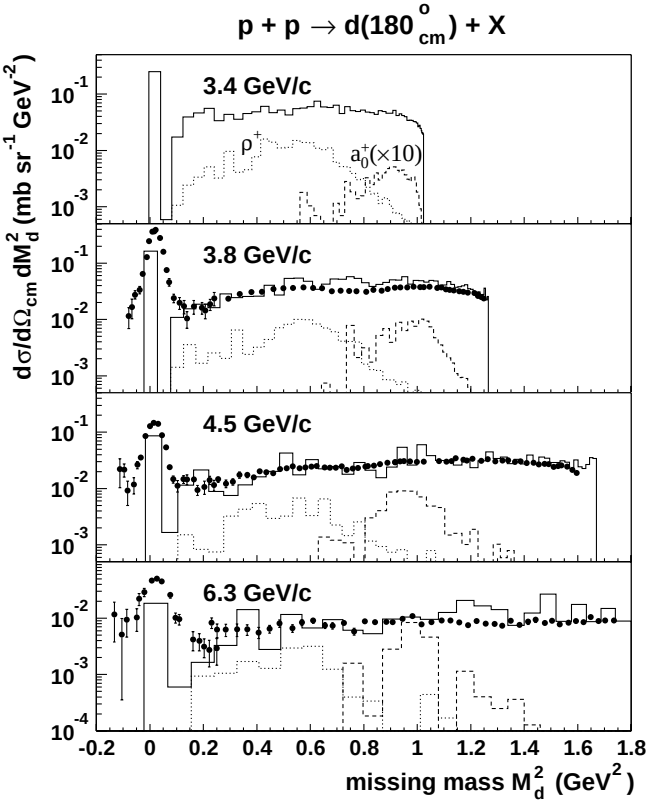

Fig. 3. The results from fig. 2 for laboratory deuteron momenta less than 2.1 GeV/c as a function of the missing mass squared in the c.m. system. Symbols and histograms have the same meaning as in fig. 2.

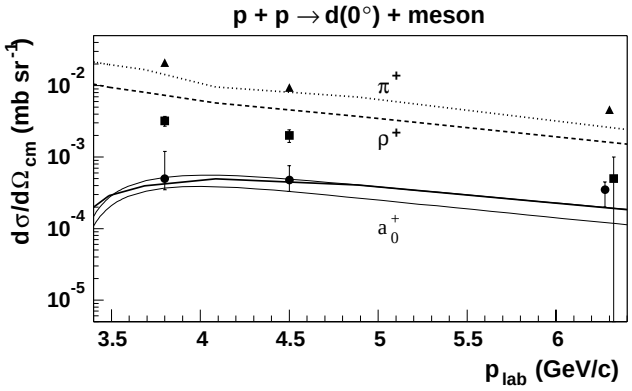

Fig. 4. Forward differential cross-sections for the reactions $p + p \to d + \pi^+$ (triangles and dotted line), $p + p \to d + \rho^+$ (squares and dashed line) and $p + p \to d + a_0^+$ (dots and full lines). The symbols denote the data [4], the dotted, dashed and thick full lines ROC model calculations, and the two thin full lines are the results of [2] for $p + p \to d + a_0^+$. All results are plotted as a function of the laboratory momentum $p_{\rm lab}$. The data points for ρ^+ and a_0^+ at $p_{\rm lab} = 6.3$ GeV/c are drawn with a small offset relative to their nominal momentum position to make the error bars better visible.

the production of a_0^+-mesons have been extracted from the reaction $pp \to d(0^\circ)X$ by searching for structures in the missing mass spectra derived from the measured deuteron momentum spectra. The momentum spectra are shown in fig. 2 together with ROC model calculations. Deuterons have been measured at laboratory momenta between 1.1 and 1.9 GeV/c. The most prominent features of these data are the distinct peak from the reaction $p + p \to d + \pi^+$ and a broad bump due to $p + p \to d + \rho^+$ above a slowly varying background. Evidence for a second weak enhancement identified as signal from a_0^+ production has been found too.

In the spectra calculated for a momentum interval extending beyond the measured range the two peaks from the reaction $pp \to d\pi^+$ with the deuteron either forward or backward emitted in the c.m. system are clearly visible (the forward peak is outside the plotted momentum interval for the incidence momentum of 6.3 GeV/c). The interesting ρ^+ and a_0^+ contributions are shown separately with the a_0^+ regions multiplied by a factor of 10. In fig. 3 the low momentum region of fig. 2 is stretched by plotting the results as functions of the missing mass squared for laboratory deuteron momenta less than 2.1 GeV/c. This momentum region corresponds to backward emission of deuterons in the c.m. system.

The comparison of the measured and the calculated spectra verifies that the model yields a reasonable description of the sum of all the background processes in the a_0^+ region. The upper panels of figs. 2 and 3 show predictions for the highest incident momentum reachable at COSY, namely 3.4 GeV/c. From fig. 3 it can be deduced that finding an a_0^+ signal in an inclusive deuteron measurement at COSY is more difficult than at higher energies due to the higher background. In addition, a possible a_0^+ signal is near the phase-space boundary. This makes a background subtraction even more difficult. Thus, at lower energies one has to rely on correlation measurements to suppress the background.

In fig. 4 the forward differential cross-sections for π^+, ρ^+ and a_0^+ production from the inclusive deuteron measurements [4] are shown together with the results of ROC model calculations. All data points are reproduced within a factor of about two. For comparison the results of [2] for a_0^+ production are shown (the two thin full lines) which are calculated in the framework of the two-step model (TSM). TSM and ROC results agree reasonably well in the considered momentum region.

4 Discussion

The following considerations aim at giving an estimate of the physical background which must be expected when searching for the a_0^+. We consider ANKE at COSY (Jülich) and HADES at SIS (Darmstadt). In the calculations, the acceptance of the apparatus is approximated by cuts in the polar angle, $\Theta \leq 10^\circ$ for ANKE and $5^\circ \leq \Theta \leq 40^\circ$ for HADES. A momentum resolution of 1.5% is modeled by adding to each calculated three-momentum $\mathbf{p}$ of a charged particle a random momentum

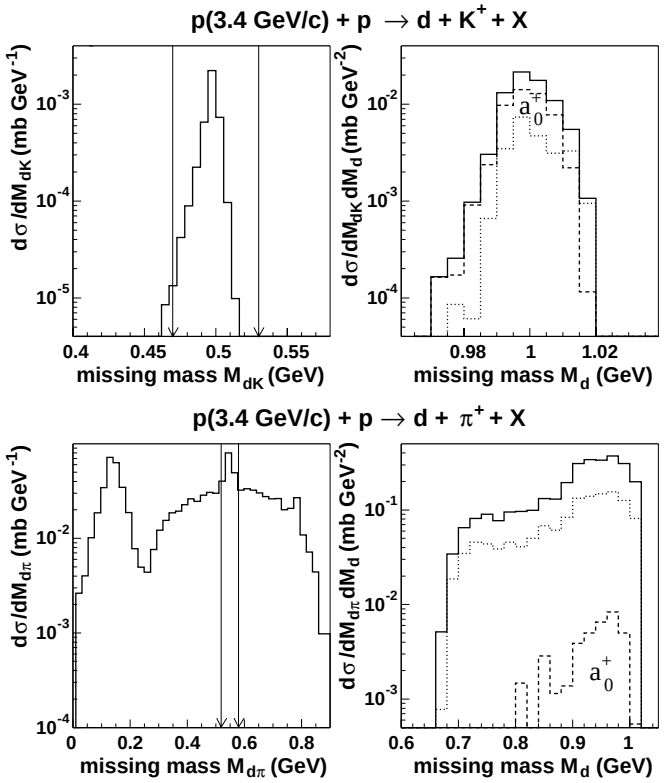

Fig. 5. Missing mass distributions for the reactions $pp \to dK^+X$ (upper panels) and $pp \to d\pi^+X$ (lower panels) calculated at incidence momentum 3.4 GeV/c for polar angles $\Theta \leq 10^\circ$ and 1.5% momentum resolution. The two arrows in the left-hand panels indicate the windows in the M_{dK} and $M_{d\pi}$ distributions, which are used in the calculation of the M_d distribution shown in the right-hand panels. The dashed histograms indicate the contributions from the reaction $pp \to da_0^+$, the dotted histograms those of the non-resonant channels $pp \to dK^+\bar{K^0}$ and $pp \to d\pi^+\eta$, respectively.

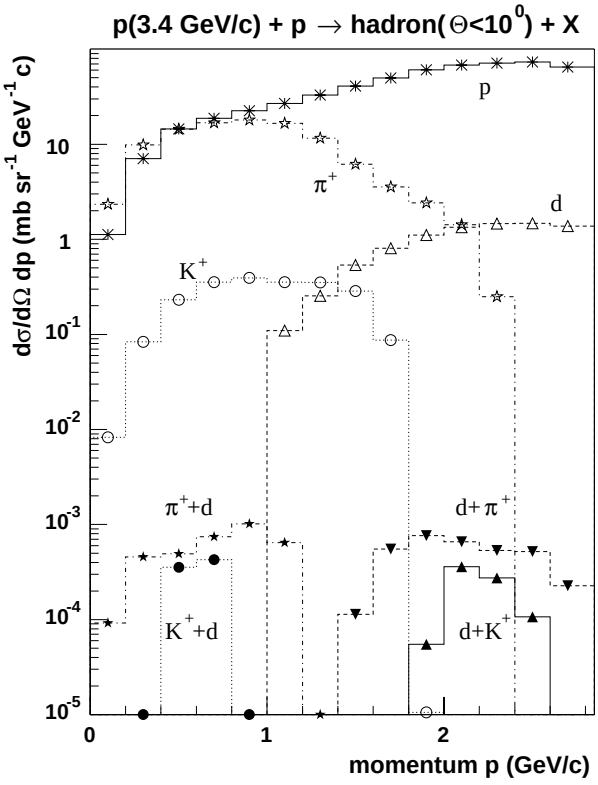

Fig. 6. Calculated differential cross-sections for the inclusive production of p, d, π^+ and K^+ compared to the calculated cross-sections from a_0^+ production. The notation $\pi^+ + d$ is used for the differential cross-section of π^+ production from the reaction $pp \to da_0^+ \to d\eta\pi^+$ in coincidence with the d. Both particles are emitted at angles $\Theta \leq 10^\circ$. Analogous notations are used for the other two-particle combinations. The momentum distributions are shown for the first particle with the second one in coincidence as trigger condition. The various histograms are distinguished by different line and marker types.

sampled from a Gaussian distribution with rms deviation $\sigma = 0.015 \times |\mathbf{p}|$.

In fig. 5 the calculated missing mass distributions at the highest COSY momentum, 3.4 GeV/c, are shown. The squared missing mass of $d + K^+$ is defined by $M_{dK}^2 = (p - p_d - p_{K^+})^2$, that of $d + \pi^+$ by $M_{d\pi}^2 = (p - p_d - p_{\pi^+})^2$ and that of d by $M_d^2 = (p - p_d)^2$ with p being the total four momentum and p_d, p_{K^+} and p_{π^+} the four momenta of the deuteron, the K^+ and the π^+-mesons, respectively. The missing mass distributions of two particles are used to select the mass of the third particle defining thus the final channel. Then the signal from the a_0^+ is looked for in the missing mass distribution of M_d. In case of strangeness production there are no background reactions, while channels with three or four pions may contribute to the η window in the $M_{d\pi}$ distribution. One of them is detected, the other two or three may have an invariant mass lying within the η window. The difference between the full and the dotted histogram in the lower right panel of fig. 5 is the contribution from these pion channels, which is of the same order as the contribution from the non-resonant channel $pp \to d\pi^+\eta$ (the dotted histogram). Usually, one gets rid of this type of background by selecting additional windows of both sides of the η peak and subtracting these spectra from the spectrum with the window on the η peak.

The main difficulty consists, however, in differentiating between the channels via the a_0^+-meson and the channels with non-resonant production. Ideally, one has the resonant signal above a smooth non-resonant background. In case of broad resonances it becomes more and more difficult to identify the signal, and if the measurable mass region is small compared to the resonance width, then a model independent determination of the resonance contribution becomes extremely difficult. This is the case for the channel $pp \to dK^+\bar{K^0}$, where the missing mass M_d varies by about half the assumed width of the a_0^+-meson.

Nevertheless, the measurement of the cross-section would yield information on the nature of the a_0 (see also the discussion on this point in [2]). The value of the calculated cross-section for a_0^+ production is closely related to the assumption that the a_0^+ has a strong $u\bar{d}$

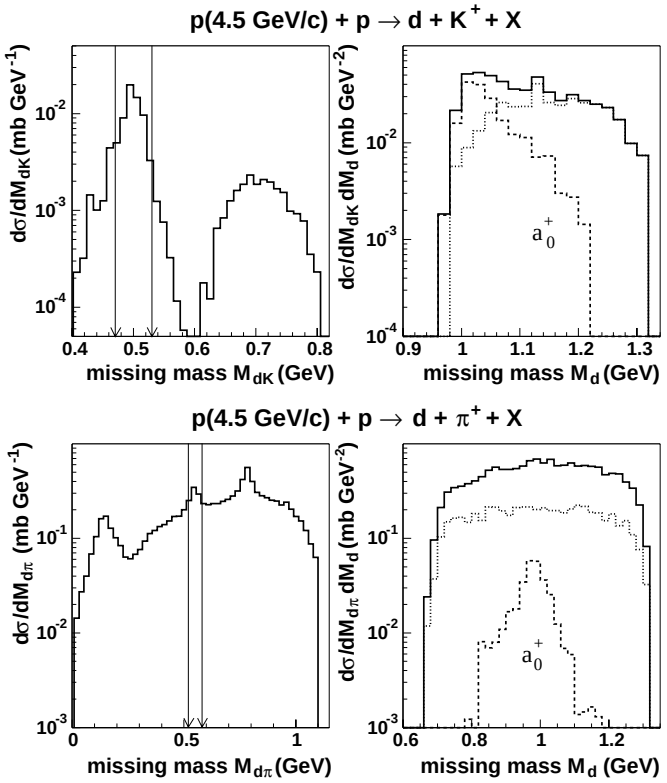

Fig. 7. The same as fig. 5 for 4.5 GeV/c and angular interval $5^\circ < \Theta < 40^\circ$.

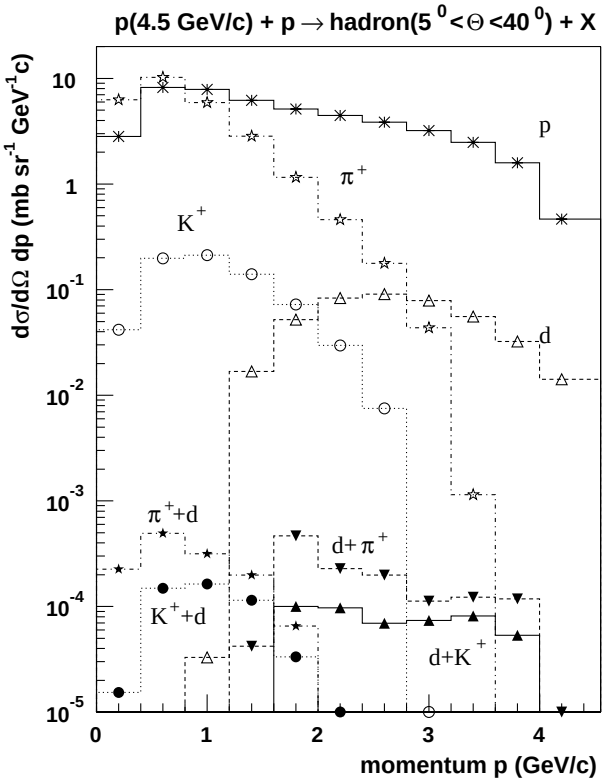

Fig. 8. The same as fig. 6 for 4.5 GeV/c and angular interval $5^\circ < \Theta < 40^\circ$.

component. Its production in pp collisions proceeds via the creation of a $d\bar{d}$ pair. For the direct population of the channel $pp \to dK^+\bar{K^0}$ the creation of a $d\bar{d}$ and a $s\bar{s}$ pair is necessary. Strange quark production is suppressed by nearly one order of magnitude compared to that of light quarks. This causes the large contribution of an intermediate a_0^+ to the final channel $dK^+\bar{K^0}$. On the other hand, considering for example the a_0 as a $K\bar{K}$ molecule, its production would proceed via the production of a $K\bar{K}$ meson pair with subsequent final-state interaction leading to the formation of the molecule. Such a process, however, has a much lower cross-section than the values depicted in fig. 5.

In case of the decay channel, $a_0^+ \to \pi^+\eta$, the ROC model predicts higher cross-sections for the non-resonant channel than for the a_0^+ production itself. The final channel $d\pi^+\eta$ can be populated via the creation of two light quark pairs or the creation of one quark pair together with the production of a baryon resonance. A considerable contribution arises from the production of $N(1535)$ and Δ resonances without additional quark pair creation according to

$$pp \to N(1535)\Delta \to N\eta N\pi \to d\pi^+\eta\,.$$

In order to create a deuteron via coalescence, the decay of the two primarily produced resonances must proceed such that the two nucleons come close together in momentum space. This condition causes the two mesons from the decaying resonances to have in turn a large invariant mass. Thus, we have not only a large background for a_0^+ production, but, in addition, the rather unpleasant feature that the missing mass distributions of the a_0^+ channel and of the background are rather similar. This makes a separation of the a_0^+ contribution even more difficult (see the lower right-hand panel of fig. 5).

Figure 6 illustrates the problem one has usually to cope with when searching for a small effect. The inclusive particle yields are about 3 to 4 orders of magnitude larger than the yields which originate from a_0^+ production. The apparatus has to digest a high flux of particles in order to get a reasonable counting rate for a_0^+ production. Such a high particle flux may cause additional background. A detailed discussion of this problem is, however, beyond the scope of the present paper and needs a careful simulation of the whole experiment. The larger angle interval considered here compared to the results shown in fig. 2 is the reason why the peak from the binary reaction $pp \to d\pi^+$ is completely smeared out. Also the two bumps from a_0^+ production with the d emitted forward and backward in the c.m. system fuse into one broad bump around 2 GeV/c (see the d distributions in coincidence with π^+- and K^+-mesons, denoted by $d + \pi^+$ and $d + K^+$ in fig. 6).

With increasing incident momentum the mass region increases in which the non-resonant background can be measured. An example is given in fig. 7, where the charged particles are detected at polar angles $5^\circ \leq \Theta \leq 40^\circ$. In case of the final channel $d\pi^+\eta$ the missing mass distribution extends on both sides well beyond the (still rather weak) a_0^+ signal. Thus, there are regions for fixing the

parameters of a fit to the background and a high statistics measurement should allow to extract the a_0^+ contribution. For the channel $dK^+\bar{K^0}$ the difficulty remains that the a_0^+ contribution at the low mass side of the missing mass spectrum overlaps with the non-resonant channel. It should be, however, possible to extract the latter contribution from the cross-section at the high mass end, where the a_0^+ contribution vanishes. This should allow at least a model dependent estimate of the a_0^+ cross-section. Nevertheless, the a_0^+ channel is rather small compared to the inclusive production rates of the considered particles (see fig. 8). The smaller inclusive cross-sections for protons and deuterons compared to those at 3.4 GeV/c are mainly due to the different angular interval over which the cross-sections are averaged. Especially for the deuterons there is a large variation of the cross-section within the considered angular region of $5^\circ \ldots 40^\circ$.

5 Conclusions

We have applied the ROC model for calculating the inclusive deuteron spectra from the reaction $pp \to dX$ at incidence momenta 3.8, 4.5 and 6.3 GeV/c. The results compare well with the available experimental data [4]. Differential cross-sections for the reactions $pp \to d\pi^+$, $pp \to d\rho^+$ and $pp \to da_0^+$ are reasonably reproduced, too. On this basis we estimate a_0^+ production under different experimental conditions together with accompanying background reactions and inclusive particle yields. The main problem for measuring the branching ratios of the a_0^+ is the possible presence of non-resonant contributions to the final channels, which are predicted by the ROC model to be much stronger than the a_0^+ contribution in case of the final channel $d\pi^+\eta$.

It should be, however, stressed once more that the calculated cross-sections should be considered as order of magnitude estimates. As can be seen from fig. 1 the ROC model tends to considerably overestimate some of the relevant cross-sections, and this might be true for the considered background reactions, too. At the same time, the not well-known width and decay probabilities of the a_0 strongly influence the calculated production cross-sections. Thus, the predicted ratio of a_0 production to non-resonant background is indeed rather uncertain, although a considerable background cannot be excluded. Nevertheless, it can be expected that the discussed measurements, if performed at several incident energies under different experimental conditions, should yield information on both the a_0 production cross-section as well as the a_0 branching ratios. This would be a valuable contribution towards a better understanding of the nature of the a_0-meson.

The author would like to thank M. Büscher, B. Kämpfer, L.A. Kondratyuk and especially H.-W. Barz for valuable discussions and the careful reading of the manuscript. The work is supported in part by BMBF grants 06DR920 and 06DR828/I.

References

1. C. Caso et al., Eur. Phys. J. C **3**, 1 (1998).
2. V. Y. Grishina et al., Eur. Phys. J. A **9**, 277 (2000); nucl-th/0007074.
3. V. Chernyshev et al., *COSY Proposal #55 "Study of a_0^+-mesons at ANKE"*, Jülich (1997), available via: `http://ikpd15.ikp.kfa-juelich.de:8085/doc/Anke.html`.
4. M. Abolins et al., Phys. Rev. Lett. **25**, 469 (1970).
5. H. Müller, Z. Phys. A **336**, 103 (1990).
6. H. Müller, Z. Phys. A **339**, 409 (1991).
7. H. Müller, K. Sistemich, Z. Phys. A **344**, 197 (1992).
8. H. Müller, Z. Phys. A **353**, 103 (1995).
9. H. Müller, Z. Phys. A **353**, 237 (1995).
10. H. Müller, Z. Phys. A **355**, 223 (1996).
11. H. Müller, Acta Phys. Pol. B **27**, 3385 (1996).
12. H. Müller, Eur. Phys. J. C **18**, 563 (2001).
13. R. Scheibl, U. Heinz, Phys. Rev. C **59**, 1585 (1999).
14. M. Lacombe et al., Phys. Lett. B **101**, 139 (1981).
15. A. Baldini et al., *Total Cross-Sections for Reactions of High Energy Particles*, in *Zahlenwerte und Funktionen aus Naturwissenschaft und Technik*, Vol. **12** (Springer-Verlag, Berlin, Heidelberg, New York, London, Paris, Tokyo, 1988).
16. H. Anderson et al., Phys. Rev. D **9**, 580 (1974).
17. M. Drochner et al., Nucl. Phys. A **643**, 55 (1999).
18. J. Balewski et al., Phys. Lett. B **420**, 211 (1998).
19. S. Sewerin et al., Phys. Rev. Lett. **83**, 682 (1999).
20. R. Bilger et al., Phys. Lett. B **420**, 217 (1998).
21. E. Chiavassa et al., Phys. Lett. B **322**, 270 (1994).
22. H. Calén et al., Phys. Lett. B **366**, 39 (1996).
23. F. Hibou et al., Phys. Lett. B **438**, 41 (1998).
24. J. Smyrski et al., Phys. Lett. B **474**, 182 (2000).
25. P. Moskal et al., Phys. Rev. Lett. **80**, 3202 (1998).
26. P. Moskal et al., Phys. Lett. B **474**, 416 (2000).
27. F. Balestra et al., Phys. Lett. B **491**, 29 (2000).
28. M. Wolke, *Schwellennahe assoziierte Strangeness-Erzeugung in der Reaktion $pp \to ppK^+K^-$ am Experiment COSY-11*, Ph.D. thesis, Rheinische Friedrich-Wilhelms-Universität Bonn (1997), ISSN 0944-2952.
29. F. Balestra et al., Phys. Lett. B **468**, 7 (1999).
30. M. Wolke, in *VII International Conference on Hypernuclear and Strange Particle Physics (HYP2000), Torino, 23-27 October 2000*, to be published in Nucl. Phys. A.
31. G. Fäldt, C. Wilkin, Phys. Lett. B **382**, 209 (1996).
32. E. Gedalin, A. Moalem, L. Razdolskaja, Nucl. Phys. A **650**, 471 (1999).
33. A. Sibirtsev et al., Tech. Rep. ADP-00-15/T399, UGI-00-7, Giessen U., CSSM, University of Adelaide, Australia (2000); nucl-th/0004022.